Available online at www.sciencedirect.com
SCIENCE DIRECT®
Bioorganic Chemistry 33 (2005) 285–297
BIOORGANIC CHEMISTRY
www.elsevier.com/locate/bioorg

Bisubstrate analog probes for the insulin receptor protein tyrosine kinase: Molecular yardsticks for analyzing catalytic mechanism and inhibitor design

Aliya C. Hines [a], Keykavous Parang [a,b], Ronald A. Kohanski [a,c], Stevan R. Hubbard [d], Philip A. Cole [a,*]

[a] *Department of Pharmacology and Molecular Sciences, Johns Hopkins University School of Medicine, Baltimore, MD 21205, USA*
[b] *Department of Biomedical and Pharmaceutical Sciences, University of Rhode Island, Kingston, RI 02881, USA*
[c] *Department of Pediatrics, Johns Hopkins University School of Medicine, Baltimore, MD 21205, USA*
[d] *Structural Biology Program, Skirball Institute of Biomolecular Medicine, New York University School of Medicine, New York, NY 10016, USA*

Received 17 January 2005
Available online 19 April 2005

Abstract

Bisubstrate analogs have the potential to provide enhanced specificity for protein kinase inhibition and tools to understand catalytic mechanism. Previous efforts led to the design of a peptide–ATP conjugate bisubstrate analog utilizing aminophenylalanine in place of tyrosine and a thioacetyl linker to the γ-phosphate of ATP which was a potent inhibitor of the insulin receptor kinase (IRK). In this study, we have examined the contributions of various electrostatic and structural elements in the bisubstrate analog to IRK binding affinity. Three types of changes (seven specific analogs in all) were introduced: a Tyr isostere of the previous aminophenylalanine moiety, modifications of the spacer between the adenine and the peptide, and deletions and substitutions within the peptide moiety. These studies allowed a direct evaluation

* Corresponding author. Fax: +1 410 614 7717.
E-mail address: pcole@jhmi.edu (P.A. Cole).

doi:10.1016/j.bioorg.2005.02.002

of the hydrogen bond strength between the anilino nitrogen of the bisubstrate analog and the enzyme catalytic base Asp and showed that it contributes 2.5 kcal/mol of binding energy, in good agreement with previous predictions. Modifications of the linker length resulted in weakened inhibitory affinity, consistent with the geometric requirements of an enzyme-catalyzed dissociative transition state. Alterations in the peptide motif generally led to diminished inhibitory potency, and only some of these effects could be rationalized based on prior kinetic and structural studies. Taken together, these results suggest that a combination of mechanism-based design and empirical synthetic manipulation will be necessary in producing optimized protein kinase bisubstrate analog inhibitors.

Keywords: Kinase; Peptide; Protein; Inhibitor; Nucleotide

1. Introduction

Protein kinase superfamily members are critical cell signal transduction enzymes that catalyze the transfer of the γ-phosphoryl group of ATP to serine, threonine, and tyrosine hydroxyls in proteins [1]. There are more than 500 protein kinases in the human genome and they all show conserved features at the sequence and three-dimensional structural levels [2]. Increased protein kinase activity occurs in a wide variety of pathologies including cancer, cardiovascular syndromes, immune diseases, endocrine disorders, and inflammatory conditions [3,4]. There has been an intense search for specific inhibitors of these enzymes among biomedical investigators [4]. Bisubstrate analogs may possess enhanced potency and specificity compared to ATP-only site-targeted agents, the latter being most popular among medicinal approaches at this time [5]. In principle, a limiting feature in the design of bisubstrate analogs is an incomplete understanding of the geometric and electronic features that might contribute to binding energy of such compounds to protein kinase enzymes.

In a previous report, it was found that a potent and selective inhibitor of the insulin receptor tyrosine kinase (IRK) could be generated by linking ATP to a substrate peptide derivatized with the tyrosine surrogate aminophenylalanine (compound **1**, Fig. 1) [6]. The linkage between the two substrate moieties in **1** contains a thioacetyl bridge, which was designed based on the concept that the transition state for protein kinases appears to possess considerable dissociative character. Mildvan had proposed that in a fully dissociative transition state, the reaction coordinate distance, that is the distance between the entering oxygen and the attacked phosphorus, should be 5 Å to allow for the metaphosphate to move from ADP to the side chain hydroxyl [7]. The thioacetyl spacer, which in extended conformation would lead to a 5.7 Å distance between the Tyr oxygen surrogate (nitrogen atom) and the γ-phosphorus, roughly simulates this reaction coordinate geometry. The choice of the nitrogen atom versus the more natural oxygen atom was primarily based on the fact that a hydrogen bond between the protein kinase active site base (the carboxylate ion of Asp-1132 in IRK) and the Tyr hydroxyl appeared to be important in protein kinases, based on kinetic and structural studies [8–12].

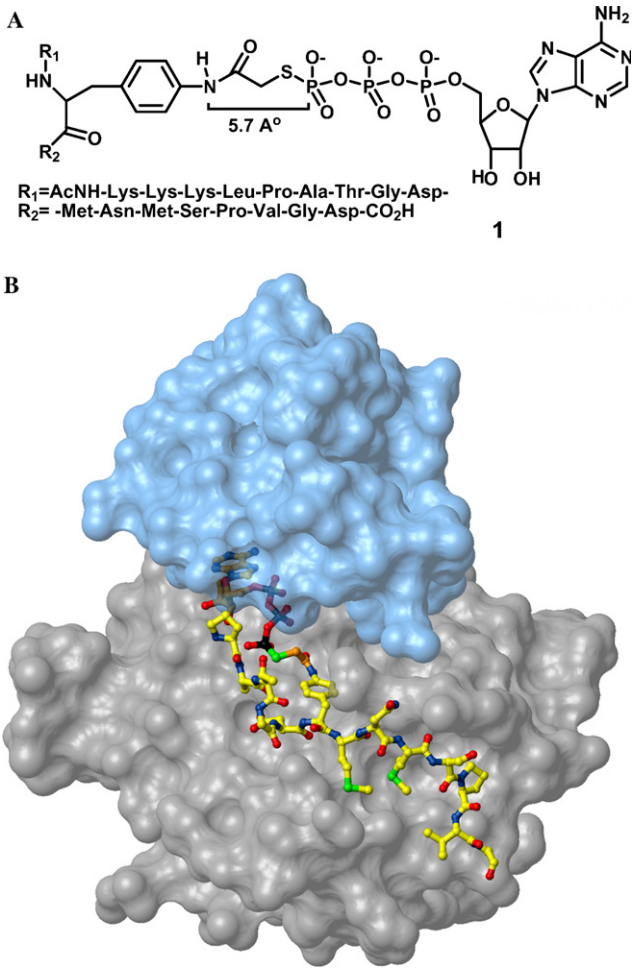

Fig. 1. (A) Structure of compound **1**. (B) Binding of compound **1** to IRK [6]. IRK is shown in molecular surface representation with atoms of the N-terminal lobe colored blue and atoms of the C-terminal lobe colored gray. The molecular surface is semi-transparent to show the ATP moiety of compound **1**. Compound **1** is show in ball-and-stick representation with nitrogen atoms colored blue, oxygen atoms colored red, sulfur atoms colored green, and phosphorus atoms colored black. Carbon atoms of the peptide moiety are colored yellow, and carbon atoms of the ATP moiety and linker are colored orange.

Kinetic analysis of bisubstrate analog **1** showed that it was a competitive inhibitor of IRK both with respect to ATP and peptide substrates with an extrapolated K_d of 400 nM, an affinity which approximates the sum of the binding energies of the peptide and ATPγS moieties individually [6]. Bisubstrate analog **1** was co-crystallized with IRK and the X-ray structure showed that both nucleotide and peptide binding sites of the enzyme were occupied by bisubstrate analog **1** and that the distance between the γ-phosphorus and the anilino nitrogen was 5 Å [6]. In addition, a hydrogen bond between the anilino nitrogen and the catalytic Asp was observed.

Although these kinetic and structural findings appeared to validate the design principles, many unanswered questions remained about this bisubstrate analog approach for protein kinase inhibition. What are the key aspects of compound **1** that are actually important for potency? How much does the hydrogen bond strength between the bisubstrate analog's anilino nitrogen and Asp-1132 contribute to affinity? Much has been proposed about this hydrogen bond in catalysis but little experimental work has evaluated its energetic contribution. Another question is how critical is the distance between the peptide and nucleotide for potent inhibition? A dissociative mechanism would predict that significant shortening might be deleterious for inhibition [7]; what about the effect of lengthening? We also wished to examine how important were the amino acids of the peptide substrate moiety in yielding potent inhibitors. In this manuscript, we have attempted to address these questions and describe our findings below.

2. Materials and methods

2.1. Peptide–ATP conjugate synthesis

All peptides were synthesized using the Fmoc strategy by solid phase peptide synthesis on a Rainin PS3 automated synthesizer employing Wang resin within a scale range of 0.1–0.3 mmol analogously to the previous method [6]. Peptides were N-terminally acetylated and, except for **2**, were prepared with a nitrophenylalanine residue replacing the target tyrosine in the peptide. After amino acid couplings, this tyrosine analog was then reduced to aminophenylalanine using a 10-fold excess of $SnCl_2$ in DMF, mixed at room temperature for 18 h [6].

Compound **2** was prepared using tyrosine carrying a 2-chlorotrityl protective group on its phenolic oxygen that was removed after amino acid couplings by orthogonal deprotection with a solution containing 1% trifluoroacetic acid and 5% triisopropylsilane in methylene chloride for 5 min followed by evaporation under a stream of N_2 (three cycles).

After side chain deprotection (for **2**) or reduction (**1**, **3**–**8**), the resin-linked peptides were serially rinsed with 10 ml, respectively, of DMF, methanol, methylene chloride, and 1:1 methylene chloride:triethylamine and then dried under vacuum. The resin-linked peptides were then reacted with either bromoacetyl bromide (for **2**), bromopropionic acid (for **3**), or bromoacetic acid (**1**, **4**–**8**). Bromoacetic acid derivatization was carried out as described previously [6]. For compound **2**, the peptide-linked resin (0.1 mmol) was treated with 0.4 ml $BrCH_2COBr$, 1 ml triethylamine, and 4 ml anhydrous methylene chloride under a N_2 atmosphere for 1 h. The peptide-linked resin was then serially washed with 10 ml of DMF, methanol, and methylene chloride, respectively. For compound **3**, peptide-linked resin (0.1 mmol) was treated with 500 mg 3-bromoproprionic acid along with 0.4 ml diisopropylcarbodiimide in 4 ml DMF (dry) and gently mixed for 24 h. The mixture was then serially washed with 10 ml DMF, methanol, and methylene chloride. For compounds **1** and **3**–**8**, bromoacetylated peptides were cleaved from solid support and deblocked using a mixture of trifluoroacetic

acid (5 ml), methylene chloride (1 ml), water (0.25 ml), and thioanisole (0.1 ml) for 2–4 h at room temperature. For compound **2**, the bromoester peptide was cleaved from solid support and deblocked using a mixture of trifluoroacetic acid (5 ml), triisopropylsilane (0.125 ml), and methylene chloride (0.125 ml) for 4 h at room temperature (Figs. 2 and 3).

The samples were filtered (Biorad poly-prep chromatography columns) to remove resin and the filtrates were collected and precipitated with chilled diethyl ether (4 °C). Mixtures were centrifuged (3000*g*), supernatants removed, and then precipitates washed again with chilled ether. Pellets were then resuspended in water and then lyophilized to dryness. Bromopeptides were purified using HPLC (Varian semi-preparative C-18 reversed phase column, methacrylate polymer sphere resin) using gradients of water/acetonitrile containing 0.05%(v/v) trifluoroacetic acid, UV monitored at 214 nm. Purified bromopeptides (concentration range 1–2.5 mg/ml in water, pH ~5) were then mixed with either ATPγS (Boehrinnger) or ADPβS (Sigma) present at 10-fold excess for 18 h at room temperature (except for compound **3** which was mixed for 48 h). Final bisubstrate analog compounds **1**–**8** were purified directly from the reaction

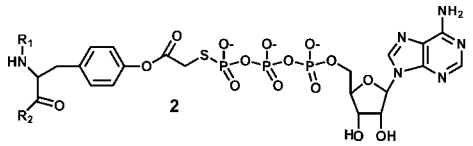

2

R_1=AcNH-Lys-Lys-Lys-Leu-Pro-Ala-Thr-Gly-Asp-
R_2= -Met-Asn-Met-Ser-Pro-Val-Gly-Asp-CO_2H

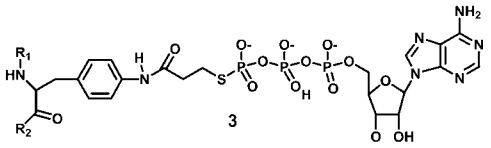

3

R_1=AcNH-Lys-Lys-Lys-Leu-Pro-Ala-Thr-Gly-Asp-
R_2= -Met-Asn-Met-Ser-Pro-Val-Gly-Asp-CO_2H

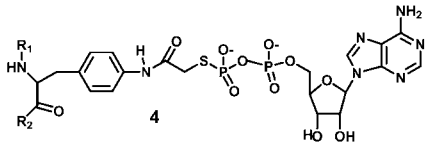

4

R_1=AcNH-Lys-Lys-Lys-Leu-Pro-Ala-Thr-Gly-Asp-
R_2= -Met-Asn-Met-Ser-Pro-Val-Gly-Asp-CO_2H

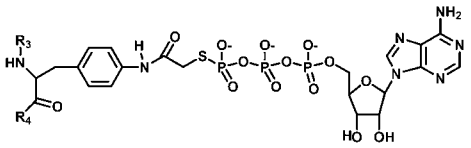

5: R_3=AcNH-Arg-Glu-Glu-Thr-Gly-Ser-Glu-Glu
R_4= -Met-Asn-Met-Asp-Leu-Gly-CO_2H

6: R_3=AcNH-Leu-Pro-Ala-Thr-Gly-Asp-
R_4= -Met-Asn-Met-Ser-Pro-Val-Gly-Asp-CO_2H

7: R_3=AcNH-Lys-Lys-Lys-Leu-Pro-Ala-Thr-Gly-Asp-
R_4= -Met-Asn-Met-Ser-CO_2H

8: R_3=AcNH-Lys-Lys-Lys-Leu-Pro-Ala-Thr-Gly-Asp-
R_4= -Met-Asn-Thr-Ser-Pro-Val-Gly-Asp-CO_2H

Fig. 2. Structures of synthetic compounds **2**–**8**.

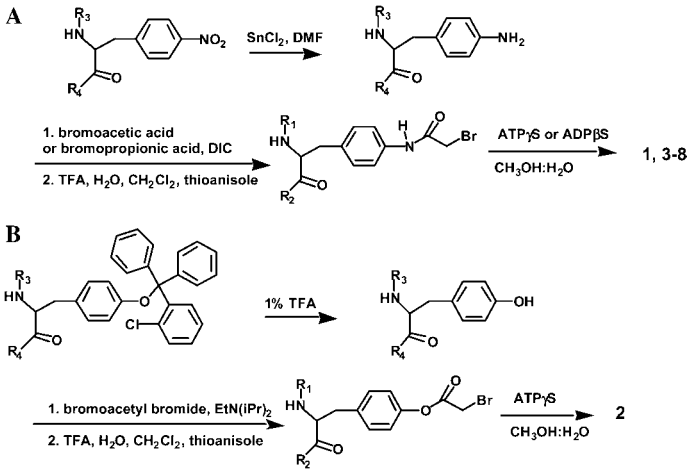

Fig. 3. Synthetic schemes for compounds **2**–**8**.

mixtures using semi-prep reversed phase HPLC (gradient, water:acetonitrile without trifluoracetic acid, UV monitored at 260 and 214 nm). Products were estimated to be greater than 90% pure by HPLC and the structures were confirmed using electrospray mass spectrometry. Product amounts were verified by measuring UV absorbance at 260 nm and by amino acid analysis (Harvard microchemistry facility).

2.2. IRK preparation

Recombinant IRK catalytic domain was expressed and purified from a baculovirus expression system in autophosphorylated (activated) form as described previously [13]. Concentration was determined by Bradford assay.

2.3. IRK kinetic assays

IRK kinase activity assays to measure inhibitor potency involved a direct radioactive assay employing [γ-^{32}P]ATP, biotinylated 727 substrate peptide (Biotin/*N*-Lys-Lys-Lys-Leu-Pro-Ala-Thr-Gly-Asp-Tyr-Met-Asn-Met-Ser-Pro-Val-Gly-Asp), and avidin binding. The reaction conditions included the following: ATP (100 μM), substrate peptide (125 μM), Mg-acetate (20 mM), IRK (5 nM), Tris–acetate (50 mM; pH 7.0), bovine serum albumin = 0.2 mg/ml, DTT (0.5 mM) in a final reaction volume of 15 μl. IRK and inhibitor were preincubated together for 10 min on ice before being added to a substrate mixture to initiate the reaction at 30 °C. Reactions were allowed to proceed for 15 min and then quenched with 10 μl of Na–EDTA (300 mM). Quenched reactions were treated with 8 μl avidin solution (Calbiochem) and incubated at room temperature for 5 min. Twenty microliter aliquots of the avidin-treated mixtures were then loaded onto microcentrifuge spin filter columns (designed for kinase assays, Calbiochem) and washed with 50 μl wash solution (Calbiochem), then centrifuged at 13,000*g* for 5 min. Columns were washed three more times with 100 μl wash solution and then inserted

into scintillation fluid (9 ml) for radioactive counting. All data were obtained with less than 10% turnover of the limiting substrate. Kinase activity was shown to be linear for at least 20 min under the conditions of the assay. All assays were performed at least twice and duplicates typically agreed within 20%. The apparent K_m values for ATP (75 μM) and peptide (293 μM) and the apparent k_{cat} value (20 s^{-1}) were in good agreement with those obtained under similar conditions and reported previously [6]. The following inhibitor concentrations (μM) were employed for the compounds evaluated: **1**, 1, 2.5, 5, 10, and 20; **2**, 10, 25, 50, 100, and 250; **3**, 1, 5, 20, 50, and 125; **4**, 1, 5, 10, 20, 50, 100, 250, and 400; **5**, 0.5, 1, 5, 10, and 40; **6**, 1, 5, 10, 20, and 50; **7**, 1, 5, 20, 50, and 500; **8**, 1, 5, 10, 20, and 50. IC_{50} values were obtained from Dixon plots (I/V vs. I) which displayed linear inhibitory behavior. The IC_{50} of 1 (2.37 μM) extrapolates to K_i of 800 nM assuming linear competitive inhibition versus ATP and substrate peptide, about 2-fold higher than the K_i (400 nM) determined previously [6].

3. Results

3.1. Synthesis of peptide–nucleotide conjugates

Several of the compounds (**5**–**8**) prepared followed the previously described route of Parang et al. [6], except for the different amino acid residues used for solid phase peptide synthesis. In particular, nitrophenylalanine was used as a precursor of aminophenylalanine and in the context of protected immobilized peptides was reduced with stannous chloride under acidic conditions. It is noteworthy that these conditions are compatible with Boc protected side chains as well as Wang resin. After conversion of the nitro group to the amino group, reaction with bromoacetic acid generated the corresponding bromoanilide derivatives which were cleaved from the resin and purified by reversed-phase HPLC. Coupling with ATPγS was carried out in solution phase in the presence of triethylammonium acetate buffer, pH 7 and these reactions proceeded smoothly to generate the peptide–ATP conjugates. Purification of these compounds was achieved by reversed-phased HPLC in the absence of trifluoroacetic acid, which was omitted because of the acid lability of the final compounds. However, at neutral pH, these compounds were stable indefinitely when stored at −80 °C.

Synthesis of the ester analog **2** involved two modifications compared to the amide analogs. The use of Tyr protected with a 2-chlorotrityl group on the phenolic oxygen was used in place of nitrophenylalanine. Selective removal of the 2-chlorotrityl group with dilute trifluoroacetic acid was achieved. Coupling of the resin bound phenol was carried out with bromoacetyl bromide rather than the less reactive bromoacetic acid, taking into account the reduced nucleophilicity of the phenol. Interestingly, completion of the ATP conjugation reaction occurred without incident and the phenolic ester linked compound also appeared stable on storage.

The propionyl and ADP containing derivatives **3** and **4** were also prepared using similar procedures compared with the parent compound **1**, except that 3-bromopropionic acid was used in place of bromoacetic acid and ADPβS was used in place of ATPγS for **3** and **4**, respectively. The overnight coupling reaction time of the bromo-

propionanilide with ATPγS proved to be sufficient despite the reduced reactivity of the alkyl halide in the β substituted system.

3.2. Hydrogen bond strength evaluation in IRK inhibition by 1

To assess the contribution of a hydrogen bond involving the anilino nitrogen of compound **1** to its overall affinity, analog **2** was examined. Analysis of compound **2** as an inhibitor of IRK indicated that it was approximately 80-fold weaker than the parent compound **1** as shown in Table 1. This inhibitory potency reflects a loss of approximately 2.5 kcal/mol in decreased binding energy compared to **1**, establishing the critical importance of the Asp-1132-anilino hydrogen bond to this interaction (Fig. 4). Note that this energetic term will be composed of a favorable (hydrogen bonding) interaction as well as the absence of a potentially unfavorable interaction found in the **2**-IRK complex (electrostatic repulsion between the oxygen lone pair of **2** and the Asp-1132 carboxylate) [14]. Of course, to the extent that Asp-1132 may exist partially as the neutral carboxylic acid at pH 7, this repulsion will be offset. Moreover, subtle geometric differences between the ester and amide may also contribute to the binding energy differences.

In any case, the energetic value of 2.5 kcal/mol is indicative of an important hydrogen bond, but not as large as some "short, strong" hydrogen bonds described in some other enzyme–ligand interactions [15–19]. However, it is in the range expected based on two previous reports, one experimental [11], and one theoretical [20]. In the previous experimental study in which the pK_a of the substrate tyrosine hydroxyl was found to be elevated 2 U compared to free solution, a 2.8 kcal/mol hydrogen bond to the catalytic Asp was deduced [11]. In a recent computational analysis on protein kinase A, the hydrogen bond strength was increased 2 kcal/mol in the transition state versus the ground state [20]. This 2 kcal/mol increase is most likely directly comparable to the 2.5 kcal/mol representing the difference in affinity of **1** versus compound **2** to IRK.

3.3. Linker distance analysis for IRK inhibition

To determine the importance of the linker distance, two new compounds **3** and **4** have been prepared which have longer or shorter distances between the peptide and

Table 1
Inhibitory values for peptide–nucleotide conjugates

Bisubstrate analog	Structural modification	IC_{50} (μM)
1	Parent compound	2.37
2	Ester linkage	175
3	Linker methylene insertion	42
4	Phosphate removal	>500
5	IRS 939 peptide sequence	9.9
6	N-terminal truncation	14.9
7	C-terminal truncation	10.5
8	Met/Thr replacement	15.2

Values shown have standard errors ±20%. See experimental procedures for full details.

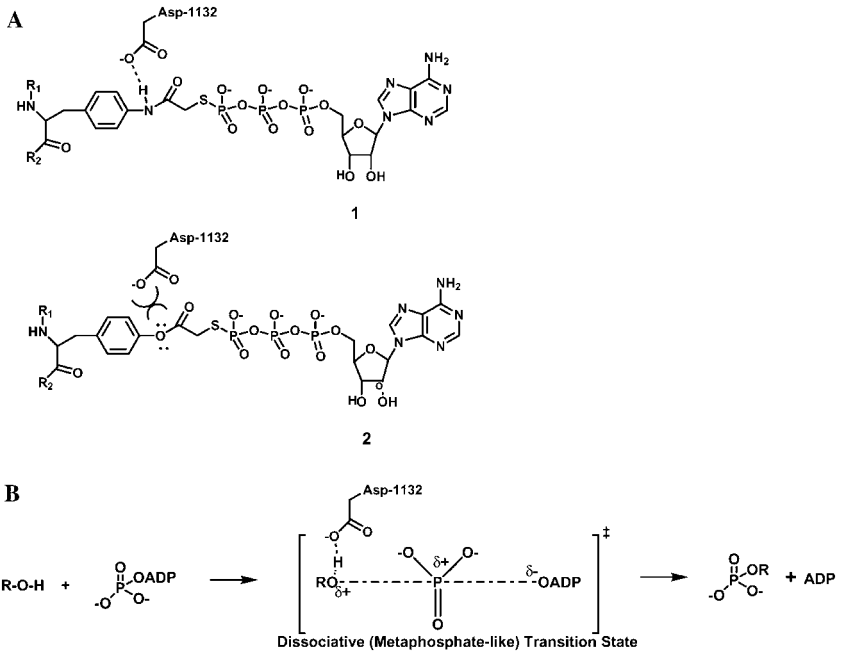

Fig. 4. Role of Asp-1132 of IRK in binding and catalysis. (A) Schematic of H-bonding replaced with oxygen. (B) Asp-1132 functions to orient and activate the tyrosine for phosphoryl transfer in a dissociative transition state.

the nucleotide. The more subtle change is the insertion of a methylene group between the ATPγS and the acetyl spacer, as in bisubstrate analog **3**. Compound **4** preserves the peptide thioacetyl moiety but removes a phosphate from the triphosphate linkage with adenosine. The affinities for these compounds indicate that compound **3** is 18-fold less potent and compound **4** at least 200-fold less potent than parent compound **1**. Inevitably, it is difficult to interpret precisely the effects of linker changes because of subtle rotational freedom differences and molecular contact changes. Overall, these studies underscore, however, the importance of linker length in compound **1** for achieving high affinity interaction. Compound **4**, lacking a phosphate, brings the adenosine moiety about ~4 Å closer to the anilino nitrogen. This distance shortening may approximate the effect of removal of the acetyl spacer between ATP and peptide. This close apposition of the two substrate moieties could perhaps mimic the geometry of a highly associative transition state [7]. Its lack of potent inhibition is therefore consistent with the proposal that protein kinases follow mechanisms with considerable dissociative character. Ideally, we could have introduced a more subtle perturbation such as removal of a methylene from the acetyl spacer. However, such compounds are unlikely to show sufficient stability to permit enzymatic analysis.

The rather substantial reduction in affinity of compound **3** for IRK compared with compound **1** was somewhat unexpected. The effect of methylene insertion in compound **3**, corresponding to a ~1.2 Å lengthening of the linker compared with **1**,

indicates that compound **1** maximizes the distance necessary to achieve potent inhibition by bisubstrate analogs for IRK, and by extension other protein kinases. This finding supports the concept of a geometric boundary on substrate alignment in the catalytic mechanisms of protein kinases, even as they appear to utilize dissociative transition states to facilitate phosphoryl transfer.

3.4. Peptide sequence analysis for IRK inhibition

The presence of the specific amino acids in compound **1** has been suggested to be critical for IRK inhibition [6] and here we analyze their importance by preparing derivatives **5**–**8**. These compounds investigate the length of the peptide on the N- and C-terminal sides as well as specific residues that from previous kinetic and structural studies appear to be important for recognition. As can be seen in Table 1, removal of either the N- or C-terminal residues as exemplified by compounds **6** and **7** results in significantly reduced affinity compared with parent compound **1**. The 4–5-fold loss of affinity with C-terminal truncation occurring with compound **7** can be rationalized based on interactions of residues P + 4 of **7** with a shallow groove in IRK bounded by the activation loop and α-helices EF and G observed in the X-ray structure of **1** complexed to IRK (Fig. 5, [6]). The 6-fold reduced binding affinity of compound **6** compared to compound **1** associated with the N-terminal deletion of the three Lys residues in **1** was unexpected. The X-ray structure of bisubstrate analog **1** complexed with IRK does not show density for these Lys residues implying that they are

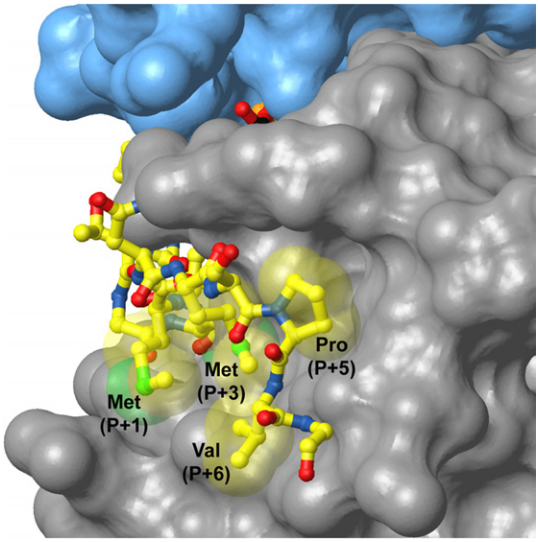

Fig. 5. Interactions of the C-terminal residues of the peptide moiety of compound **1** with IRK [6]. The molecular surface of IRK and compound **1** are colored as in Fig. 1B. The peptide moiety of compound **1** is shown in ball-and-stick representation with van der Waals spheres on the side chain atoms of Met(P + 1) (first residue C-terminal to the tyrosine surrogate), Met(P + 3), Pro(P + 5), and Val(P + 6). These residues of the peptide moiety pack against residues of the C-terminal IRK lobe. The view is approximately 90° from the right in Fig. 1B.

disordered, so no important binding role for them was predicted [6]. On the other hand, these N-terminal Lys residues may facilitate a conformation of the entire peptide moiety which is overall favorable for IRK interaction. Further studies will be needed to more fully understand the molecular basis of these findings.

A reassuring observation was the 6-fold diminished inhibitory potency of compound **8** compared with **1**. Previous enzymatic studies showed that change of the YMNM motif of IRS727 to YMNT increased the K_m of this peptide as a substrate by about 10-fold [21]. Indeed, the X-ray structure of **1** complexed with IRK demonstrates van Der Waals contacts involving the Met side chain indicative of shape complementarity at the P+3 binding pocket of the kinase [6,13]. Thus, there is a reasonably good correlation of kinetic interactions and potency in this case.

In contrast, compound **5** which contains the IRS939 amino acid sequence made a weaker bisubstrate analog than expected, being 4-fold less potent than parent compound **1**. Previous kinetic experiments with IRK suggested that the IRS939 sequence is a more efficient substrate for IRK than the IRS727 peptide [22]. Taken together with the above, these results point to the possibility that peptide substrate processing efficiency per se does not fully predict potency and specificity of bisubstrate analogs as kinase inhibitors, and that exploring further sequence diversity may lead to the most powerful inhibitors.

4. Discussion

Determining the degree of associative versus dissociative character for phosphoryl transfer reactions catalyzed by enzymes continues to be a vexing problem in mechanistic biochemistry [8–12,23–30]. Initially, when the X-ray structure of protein kinase A showed a cluster of positively charged groups coordinating to the γ-phosphate of ATP to make it a better electrophile, an associative transition state model was proposed for protein kinases [31]. Alternatively, linear free energy relationship studies and reaction coordinate distances favored a dissociative model for the superfamily of enzymes [9,10]. The role of the catalytic Asp as base in the reaction has been debated, with arguments favoring an associative model if early deprotonation of the Ser/Tyr is required and a dissociative model if late deprotonation occurs [8–11,20,31].

Previous efforts to successfully design a potent and selective bisubstrate analog in which a ~5 Å spacer was inserted between ATP and peptide provided independent experimental evidence for the dissociative catalytic mechanism of protein kinases [6]. Other recent protein kinase crystal structures are also generally consistent with this model [32,33]. In the current study, these findings have been more fully developed to assess the predictive value of the earlier work. Perhaps most significantly, a direct measurement of the hydrogen bond strength between the bisubstrate analog and the catalytic base was obtained. This value correlated well with energetic predictions based on prior indirect experiments and theoretical calculations [10,11,20].

The linker in **1** was predicted to approximate the reaction coordinate distance of 5 Å between the entering oxygen and the attacked phosphorus, proposed for a dissociative transition state. In the current study, the importance of this linker length was probed and both longer and shorter linkers failed to match the potency conferred

with the linkage in **1**. While the comparison between **1** and **4** is more complicated because of the difference in number of phosphates, a significant body of data on nucleotide analogs has suggested that the principle source of affinity of nucleotides for kinases comes from the adenine group rather than the ribo-phosphate moieties [5,34–36]. Thus, it is fair to hypothesize that, to a first approximation, the reduced affinity of **4** for IRK relates to its poor mimicry of a dissociative transition state reaction coordinate distance. Previous studies on a bisubstrate analog with a short linker, with direct connection of the Ser oxygen atom to the γ-phosphate of ATP, targeting the Ser/Thr protein kinase A gave a similarly weak inhibitor in that system [37]. Taken together, the results with inhibitors **2**–**4** are consistent with a phosphoryl transfer mechanism of Fig. 4b displaying the key features of hydrogen bonding and pronounced leaving group departure.

The crystal structure of **1** bound to IRK [6] leads to some predictions into the role of peptide sequence and its relationship to affinity. Here, we investigated the role of sequence selectivity by synthesizing several compounds containing either deletions or replacements of amino acid residues in the inhibitor. While the prior crystal structure was useful in rationalizing some of the effects observed, other affinity changes were not readily understood from prior kinetic or structural data and point to a continued role for empirical synthetic diversification in these systems.

Given the apparent generalizability of the original bisubstrate inhibitory approach on IRK to the serine/threonine kinase protein kinase A [38], and the tyrosine kinase Csk [39], it is likely that the structure–activity relationships uncovered here will show relevance to a myriad of other protein kinases. Thus, the original design strategy of linker length and hydrogen bond considerations that led to compound **1** remains the optimal starting point for potent protein kinase bisubstrate analog inhibitors.

Acknowledgments

We thank the NIH (DK052916 (S.R.H.), CA74305 (P.A.C.)), the Packard, Pfeiffer, and UNCF Merck program foundations (A.C.H.) for financial support and Cole lab members for helpful suggestions.

References

[1] C.M. Smith, I.N. Shindyalov, S. Veretnik, M. Gribskov, S.S. Taylor, L.F. Ten Eyck, P.E. Bourne, Trends Biochem. Sci. 22 (1997) 444–446.
[2] G. Manning, D.B. Whyte, R. Martinez, T. Hunter, S. Sudarsanam, Science 298 (2002) 1912–1934.
[3] P. Blume-Jensen, T. Hunter, Nature 411 (2001) 355–365.
[4] P. Cohen, Nat. Rev. Drug Discov. 1 (2002) 309–315.
[5] K. Parang, P.A. Cole, Pharmacol. Ther. 93 (2002) 145–157.
[6] K. Parang, J.H. Till, A.J. Ablooglu, R.A. Kohanski, S.R. Hubbard, P.A. Cole, Nat. Struct. Biol. 8 (2001) 37–41.

[7] A.S. Mildvan, Proteins 29 (1997) 401–416.
[8] J. Zhou, J.A. Adams, Biochemistry 36 (1997) 2977–2984.
[9] K. Kim, P.A. Cole, J. Am. Chem. Soc. 119 (1997) 11096–11097.
[10] D.M. Williams, P.A. Cole, J. Am. Chem. Soc. 124 (2002) 5956–5957.
[11] A.J. Ablooglu, J.H. Till, K. Kim, K. Parang, P.A. Cole, S.R. Hubbard, R.A. Kohanski, J. Biol. Chem. 275 (2000) 30394–30398.
[12] D. Wang, P.A. Cole, J. Am. Chem. Soc. 123 (2001) 8883–8887.
[13] S.R. Hubbard, EMBO J. 16 (1997) 5572–5581.
[14] C.C. McComas, B.M. Crowley, D.L. Boger, J. Am. Chem. Soc. 125 (2003) 9314–9315.
[15] C.N. Schutz, A. Warshel, Proteins 55 (2004) 711–723.
[16] W. Cleland, M. Kreevoy, Science 264 (1994) 1887–1890.
[17] F. Hibbert, J. Emsley, Adv. Phys. Org. Chem. 26 (1990) 255–379.
[18] B. Schwartz, D.G. Drueckhammer, J. Am. Chem. Soc. 117 (1995) 11902–11905.
[19] A.S. Mildvan, T.K. Harris, C. Abeygunawardana, Methods Enzymol. 308 (1999) 219–245.
[20] M. Valiev, R. Kawai, J.A. Adams, J.H. Weare, J. Am. Chem. Soc. 125 (2003) 9926–9927.
[21] S.E. Shoelson, S. Chatterjee, M. Chaudhuri, M.F. White, Proc. Natl. Acad. Sci. USA 89 (1992) 2027–2031.
[22] A.J. Ablooglu, R.A. Kohanski, Biochemistry 40 (2001) 504–513.
[23] I. Nikolic-Hughes, D.C. Rees, D. Herschlag, J. Am. Chem. Soc. 126 (2004) 11814–11819.
[24] J. Aqvist, K. Kolmodin, J. Florian, A. Warshel, Chem. Biol. 6 (1999) R71–R80.
[25] S.D. Lahiri, G. Zhang, D. Dunaway-Mariano, K.N. Allen, Science 299 (2003) 2067–2071.
[26] M. Forconi, N.H. Williams, Angew. Chem. Int. Ed. Engl. 41 (2002) 849–852.
[27] D.F. McCain, I.E. Catrina, A.C. Hengge, Z.Y. Zhang, J. Biol. Chem. 277 (2002) 11190–11200.
[28] G.M. Blackburn, N.H. Williams, S.J. Gamblin, S.J. Smerdon, Science 301 (2003) 1184.
[29] C. Kim, J. Haddad, S.B. Vakulenko, S.O. Meroueh, Y. Wu, H. Yan, S. Mobashery, Biochemistry 43 (2004) 2373–2383.
[30] D.D. Boehr, P.R. Thompson, G.D. Wright, J. Biol. Chem. 276 (2001) 23929–23936.
[31] Madhusudan, E.A. Trafny, N.H.. Xuong, J.A. Adams, L.F. Ten Eyck, S.S. Taylor, J.M. Sowadski, Protein Sci. 3 (1994) 176–187.
[32] Madhusudan, P. Akamine, N.H. Xuong, S.S. Taylor, Nat. Struct. Biol. 9 (2002) 273–277.
[33] A. Cook, E.D. Lowe, E.D. Chrysina, V.T. Skamnaki, N.G. Oikonomakos, L.N. Johnson, Biochemistry 41 (2002) 7301–7311.
[34] M.Y. Yoon, P.F. Cook, Biochemistry 26 (1987) 4118–4125.
[35] P.F. Cook, M.E. Neville Jr., K.E. Vrana, F.T. Hartl, R. Roskoski Jr., Biochemistry 21 (1982) 5794–5799.
[36] U. Schulze-Gahmen, J. Brandsen, H.D. Jones, D.O. Morgan, L. Meijer, J. Vesely, S.H. Kim, Proteins 22 (1995) 378–391.
[37] D. Medzihradszky, S.L. Chen, G.L. Kenyon, B. Gibson, J. Am. Chem. Soc. 116 (1994) 9413–9419.
[38] A.C. Hines, P.A. Cole, Bioorg. Med. Chem. Lett. 14 (2004) 2951–2954.
[39] K. Shen, P.A. Cole, J. Am. Chem. Soc. 125 (2003) 16172–16173.